Adsorption of a Ru(II) dye complex on the Au(111) surface: Photoemission and scanning tunneling microscopy

Louise C. Mayor, Alex Saywell, Graziano Magnano, Christopher J. Satterley, Joachim Schnadt, and James N. O'Shea

Citation: The Journal of Chemical Physics **130**, 164704 (2009); doi: 10.1063/1.3122685
View online: http://dx.doi.org/10.1063/1.3122685
View Table of Contents: http://scitation.aip.org/content/aip/journal/jcp/130/16?ver=pdfcov
Published by the AIP Publishing

Adsorption of a Ru(II) dye complex on the Au(111) surface: Photoemission and scanning tunneling microscopy

Louise C. Mayor,[1] Alex Saywell,[1] Graziano Magnano,[1] Christopher J. Satterley,[1] Joachim Schnadt,[2] and James N. O'Shea[1,a)]
[1]*School of Physics and Astronomy, University of Nottingham, Nottingham NG7 2RD, United Kingdom*
[2]*Division of Synchrotron Radiation Research, Lund University, S-221 00 Lund, Sweden*

(Received 12 November 2008; accepted 29 March 2009; published online 23 April 2009)

The adsorption of the dye molecule N3 [cis-bis(isothiocyanato)bis(2,2′-bipyridyl-4,4′-dicarboxylato)-ruthenium(II)] on the Au(111) surface has been studied using core-level and valence photoemission and scanning tunneling microscopy (STM). The dye molecules were deposited *in situ* using ultrahigh vacuum electrospray deposition. The core-level spectra reveal that the molecule bonds to the surface via sulfur atoms with no deprotonation of the carboxylic groups. The STM images show that at low coverage the molecules decorate the Au(111) herringbone reconstruction and form uniform monolayers as the coverage is increased. © *2009 American Institute of Physics*. [DOI: 10.1063/1.3122685]

I. INTRODUCTION

The dye molecule N3 [cis-bis(isothiocyanato)bis(2,2′-bipyridyl-4,4′-dicarboxylato)-ruthenium(II)] is a photoactive complex used in molecular photovoltaics, in particular dye-sensitized solar cells (DSCs).[1–3] N3, the structure of which is shown in Fig. 1, is of particular interest because it is the most efficient sensitizer found for DSCs to date.[4] In such a device—where a nanocrystalline film of a wide band gap semiconductor (such as TiO_2) is made light sensitive by adsorbing a monolayer of dye—electrons in the highest occupied molecular orbital (HOMO) of the dye are promoted to the lowest unoccupied molecular orbital (LUMO) by photoexcitation. In N3 these orbitals are located on the thiocyanate (NCS) and bi-isonicotinic acid ligands, respectively[1,5,6] (see Fig. 1). N3 has been shown to bond to the surface of TiO_2 via the deprotonation of the bi-isonicotinic acid ligand[6] to form a so-called 2M-bidentate anchor to the surface. This provides a strong chemical coupling to facilitate the charge transfer of electrons from the LUMO (which is located on this ligand) to the conduction band of the oxide. But this represents only half of the story since the process leaves a hole in the HOMO (located on the NCS ligands) which needs to replenished. In a typical DSC this is often achieved with a liquid electrolyte but recently a solid state solution to this problem was proposed by adsorbing the dye molecules onto a gold layer itself adsorbed on the TiO_2 surface.[7,8] In dyes such as N3 where the spatial distributions of HOMO and LUMO are separated onto different ligands of the molecules, this could offer a route to the efficient replenishment of electrons.

In this paper we present the results of a synchrotron-based photoemission and scanning tunneling microscopy (STM) study of the adsorption of N3 on the Au(111) surface. Previous studies on N3,[6] the N3 ligand bi-isonicotinic acid,[9,10] and other pyridine carboxylic acids[11–13] on TiO_2 have all been shown to bond to the surface via the oxygen atoms of the deprotonated carboxyl groups. On the Au(111) surface however, bi-isonicotinic acid bonds less strongly than on TiO_2, possibly via one or more carboxyl groups, but certainly without any deprotantation.[14,15] It is therefore reasonable to expect that N3 would bond to the Au(111) surface instead via the sulfur atoms of the thiocyanate ligands (NCS). Indeed, the interaction of sulfur-containing molecules with the gold surface is well established[16,17] and underpins much of the field of self-assembled monolayers. Such an adsorption geometry would place the molecule HOMO adjacent to the Au(111) surface and in the context of DSCs ideally located for electron replenishment. Since the dye molecule is thermally labile it cannot be deposited under ultrahigh vacuum (UHV) conditions by thermal evaporation, which has traditionally been a major hurdle to overcome in the application of high-resolution UHV techniques to systems such as these. Here we have instead used an UHV electrospray deposition process, which allows nonvolatile molecules to be deposited at pressures between 1×10^{-7} and 1×10^{-9} mbar. This technique has recently been used in both photoemission and STM studies,[18,19] and, most relevantly to the current study, the adsorption of N3 on a TiO_2(110) surface.[6]

II. METHOD

Photoemission spectroscopy experiments were carried out at the surface science undulator beamline I511-1 (Ref. 20) at MAX II, MAX-lab in Lund. The I511-1 end station is equipped with a Scienta R4000 electron analyzer, which was oriented with the analyzer axis in line with the light polarization vector **E**. The sample was oriented near to normal emission (NE), which corresponds to 7° off normal due to the grazing incidence geometry of the sample holder.

The photoemission measurements were performed using a single crystal Au(111) substrate of dimensions 10 mm diameter × 2.5 mm (Metal Crystals and Oxides, Ltd., U.K.).

a)Electronic mail: james.oshea@nottingham.ac.uk.

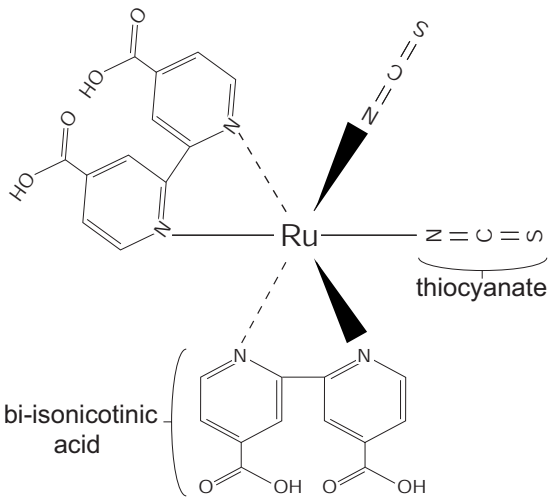

FIG. 1. Chemical structure of the N3 molecule.

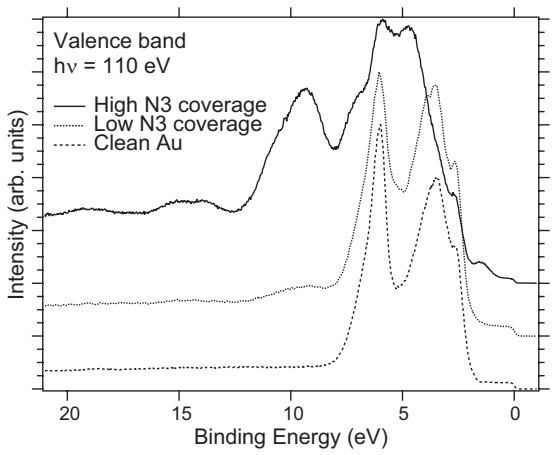

FIG. 2. Valence band photoemission spectra of clean Au and of low and high coverages of N3 on Au measured using $h\nu=110$ eV. Total instrument resolution was <65 meV.

A loop of tungsten wire was passed through the crystal, which acted as a mount and also served to heat the crystal. A thermocouple wire was attached within a small cavity in the crystal used to monitor the temperature. Cycles of sputtering using 1 keV Ar ions and annealing to ~600 °C were used to prepare the surface. The substrate was deemed clean when it showed a negligible C 1*s* core-level signal.

The N3 molecule (Solaronix SA, Switzerland) was deposited by *in situ* UHV electrospray deposition from a solution of ~5 mg of N3 in 200 ml of a 3(methanol):1(water) mixture. The apparatus used and the process by which the molecules are taken from *ex situ* solution to *in situ* vacuum are described in detail elsewhere.[6] In summary, the liquid is pushed through a hollow stainless steel needle held at ~2 kV. Here, the liquid becomes ionized and a jet emerges consisting of multiply charged droplets. The jet enters the vacuum through a series of differentially pumped chambers, in which the droplets lose solvent through evaporation and split repeatedly due to Coulomb repulsion. Between depositions, the electrospray system was sealed off from the preparation chamber using an UHV gate valve. With the valve open but the needle voltage turned off and thus no electrospray process occurring, the pressure in the preparation chamber was $\sim 2\times 10^{-8}$ mbar. With the voltage turned on, the preparation chamber pressure rose to $\sim 5\times 10^{-7}$ mbar, the additional pressure being due to residual solvent molecules in the molecular beam.

For the electron spectroscopy data, the total instrument resolution ranges from 65–195 meV. All spectra have been calibrated to the Fermi level. For the core levels, depending on the shape of the background and magnitude of the Shirley step background, a line or polynomial background was subtracted if needed before subtracting a Shirley background if necessary. Curve fitting was then performed using Gaussian functions. For all measurements, the sample was swept continuously at a rate of at least 1.25 μm/s, following beam damage studies to determine a safe exposure time.

The STM measurements were performed at Nottingham using a 4×8 mm^2 1500 Å gold on mica substrate (Agilent, USA). The sample was prepared by sputtering using 1 keV Ar ions and annealing to ~500 °C. Images of the surface were acquired using a scanning tunneling microscope housed within an UHV system using electrochemically etched tungsten tips and operating in constant current mode at room temperature.[21] Images of the surface taken after the sputter-anneal cycle show the characteristic $(22\times\sqrt{3})$ herringbone reconstruction of the Au(111) surface.[22] The N3 was then deposited onto the surface using the same UHV electrospray deposition method as above.

III. RESULTS AND DISCUSSION

Photoemission spectra were recorded for low and high coverages of N3 on Au(111), corresponding to deposition times of 15 and 30 min, respectively. Coverage is not necessarily linear with deposition time, as the electrospray process depends on many factors such that the deposition rate changes over the course of minutes. Figure 2 shows the valence band photoelectron spectra of the clean Au surface and the low and high coverages of N3 measured using $h\nu=110$ eV. It can be seen that the low coverage valence band shape is only slightly modified with respect to the valence band for clean Au. The high N3 coverage, however, has a very different shape in which the Au peaks are largely buried by the N3 molecule peaks.

Binding energies (BEs) of the x-ray photoemission spectroscopy (XPS) peaks discussed hereafter are summarized in Table I. Figure 3 shows the O 1*s* photoelectron spectra of the low and high coverages measured using $h\nu=620$ eV. Both coverages show two separate peaks at 531.4 and 533.1 eV. These are due to the O being in two different chemical environments, which are identified as the carbonyl (C=O) and hydroxyl (C–OH) groups, respectively.[9] The hydroxyl oxygen does not deprotonate at low coverages, as evidenced by the unity peak ratio. This is in contrast to the adsorption of N3 on TiO_2,[6] which shows a 3:1 peak ratio due to deprotonation of two of the carboxylic groups. The O atoms may interact with the substrate but do not form strong covalent bonds as in the case of deprotonated O atoms.

Figure 4 shows the S 2*p* photoelectron spectra of the low and high coverages measured using $h\nu=220$ eV. S 2*p* is a doublet state and here the best fits have been obtained using

TABLE I. BEs and [Gaussian FWHM] (eV) calibrated to the Fermi level.

Core level	Peak BEs and [Gaussian FWHM] (eV)				
O 1*s* both coverages	531.4[1.7]	533.1[1.9]	⋯	⋯	⋯
S 2*p* low coverage	161.0[0.5]	162.1[1.3]	164.3 [1.4]	⋯	⋯
S 2*p* high coverage	161.0[0.5]	162.1[1.1]	164.3 [1.4]	⋯	⋯
N 1*s* both coverages	396.9[1.0]	398.0[0.9]	399.9 [0.9]	⋯	⋯
C 1*s* and Ru 3*d* low coverage	280.9[0.7]	284.8[1.1]	285.8 [1.1]	287.0 [1.5]	288.6 [2.2]
C 1*s* and Ru 3*d* high coverage	280.8[0.7]	284.9[1.1]	285.7 [1.1]	286.8 [1.5]	288.6 [2.2]

a spin-orbit splitting of 1.18 eV. Both coverages require three doublets in order to obtain a good curve fit. The doublets are assigned to bonding environments by comparing the high and low coverage spectra, comparing normal and grazing emission (GE) spectra of the low coverage, and by comparison with studies of N3 on TiO_2 (Ref. 6) and atomic S on Au(111).[23]

The low BE doublet at 161.0 eV is significantly more intense for the low coverage, so it is attributed to a surface S–Au interaction. The peaks comprising the doublet are narrow with a full width at half maximum (FWHM) of 0.5 eV, implying a well-defined chemical environment. In studies of atomic S on Au(111),[23] a low BE doublet is seen at 160.8 eV, which, supported by low-energy electron diffraction studies, is attributed to S bonding to threefold hollow sites of the Au(111) surface. Since this BE is very close to that of the S–Au doublet found here at 161.0 eV, and taking into account the coverage dependence, the doublet is assigned to being due to a S–Au bond. It could also be specific to Au(111) threefold hollow sites, but further experimental investigation would be needed to confirm this.

The middle BE doublet at 162.1 eV dominates the high coverage spectrum and is also large in the low coverage spectrum. In both coverages the doublet is broad with FWHM of 1.1 and 1.3 eV for high and low coverages, respectively. These large widths imply more than one S chemical environment which have similar but unresolvable BEs. That the middle BE doublet is dominant for both low and high coverages can be accounted for if it contains a component of both nonbonded S and S bonded to Au. For atomic S on Au(111) there is a doublet at 161.6 eV corresponding to S atoms bound to Au(111) sites other than threefold hollow,[23] so it is possible that here the middle BE doublet has a similar bonded component. For N3 on TiO_2,[6] nonbonded S was found to have a BE of 161.7 eV, and the same BE would be expected here. With this peak assignment, at high coverage the middle BE doublet is expected to be mostly due to nonbonded atoms, and at low coverage a mixture of nonbonded and bonded atoms. If these components were at slightly different BEs, this would result in the low coverage having a broader FWHM than the high coverage, which is the case here.

Finally, there is a high BE doublet at 164.3 eV, which is also broad with a FWHM of 1.4 eV. Its intensity is larger at low coverage than high coverage so it is thought to be due to a surface interaction. For atomic S on Au(111), there is a

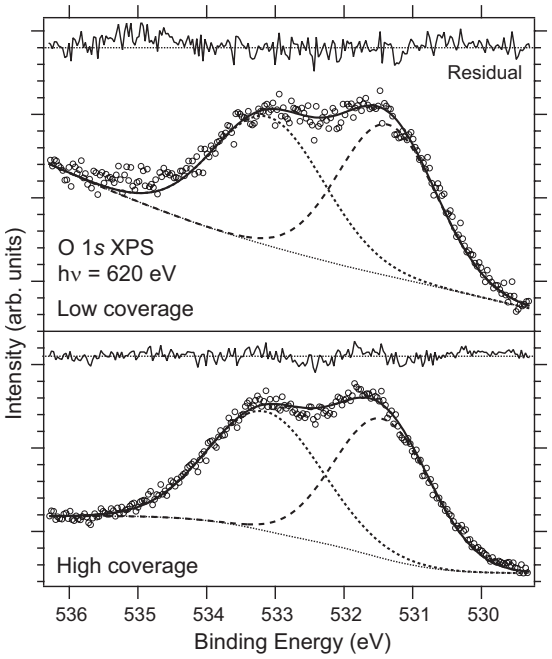

FIG. 3. O 1*s* core-level photoemission spectra measured using $h\nu$ =620 eV. Total instrument resolution was <195 meV.

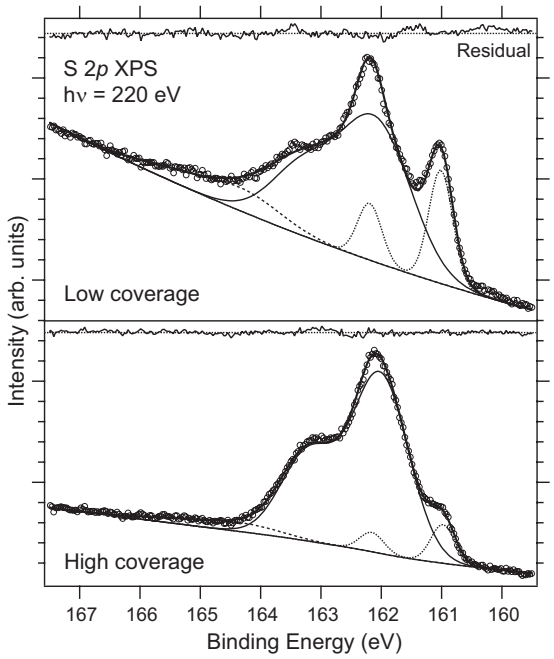

FIG. 4. S 2*p* core-level photoemission spectra measured using $h\nu$ =220 eV. Total instrument resolution was <75 meV.

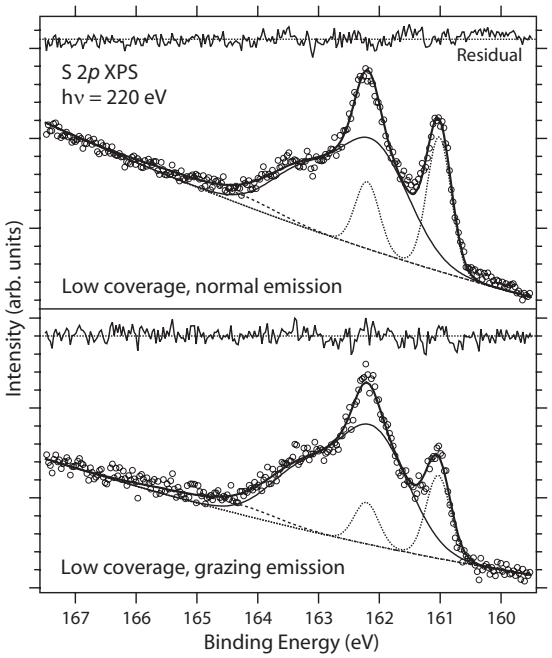

FIG. 5. S 2*p* core-level photoemission spectra comparing normal and GE measured using $h\nu$=220 eV. Total instrument resolution was <125 meV.

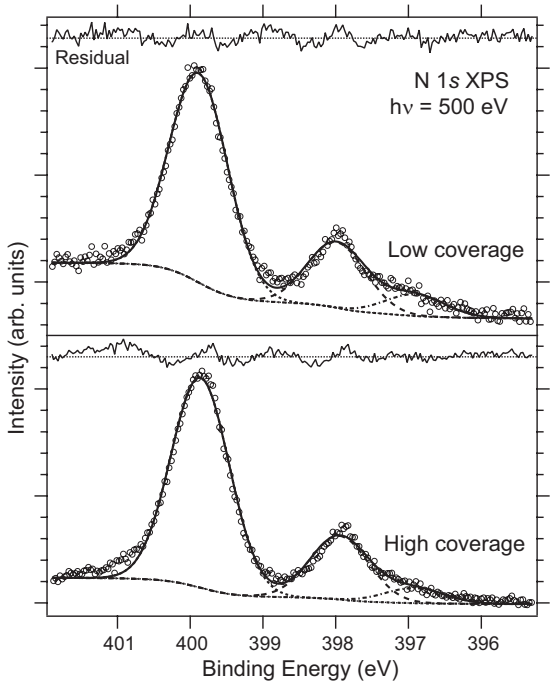

FIG. 6. N 1*s* core-level photoemission spectra measured using $h\nu$ =500 eV. Total instrument resolution was <145 meV.

high BE doublet at 163.4 eV, which at low coverage corresponds to S_2 species. It is possible that here, S atoms from different N3 molecules bond together at the Au surface. This is not unusual in the context of some alkylthiols on Au(111), which form S headgroup dimers at the surface.[16,17] Due to the geometry of the N3 molecule, we would not expect this process to occur very often on the surface, hence the low intensity of this peak.

Figure 5 shows the NE and GE S 2*p* photoelectron spectra of the low N3 coverage measured using $h\nu$=220 eV. Here NE and GE correspond to electron take-off angles of 90° and 20°, respectively, relative to the surface plane. At NE the low BE doublet is more intense than at GE, confirming that it is due to a surface interaction. The middle BE doublet has a relatively higher intensity at GE, confirming that it has a nonbonded component.

Figure 6 shows the N 1*s* photoelectron spectra of the low and high coverages measured using $h\nu$=500 eV. In N3 there are two N atoms in the bi-isonicotinic acid ligands for every one in the thiocyanate ligands. The intense, high BE peak at 399.9 eV is more than twice the intensity of the other two peaks together and is identified as the bi-isonicotinic acid N. The lower two BE peaks at 398.0 and 396.9 eV are thus attributed to the thiocyanate N. A study of N3 on TiO_2 showed the highest two of these three peaks at similar energies of 399.8 and 397.8 eV.[6] The additional low BE thiocyanate shoulder found in this case is tentatively attributed to thiocyanate N that has been shifted to lower BE due to strong chemical bonding of that thiocyanate ligand to the Au surface via the S atom.

Figure 7 shows the C 1*s* and Ru 3*d* photoelectron spectra of the low and high coverages measured using $h\nu$ =380 eV. The peak at ~280.8 eV is Ru $3d_{5/2}$ with the corresponding Ru $3d_{3/2}$ part of the doublet being hidden 4.2 eV higher[24] among the C 1*s* peaks. The remaining C 1*s* spectra have been curve fit using four peaks. Since the spectra are complicated, the FWHM of each peak has been constrained to be the same at low and high coverages, resulting in the fits shown. The pyridine and carboxyl peaks are recognizable from previous studies of bi-isonicotinic acid on Au/TiO_2.[15]

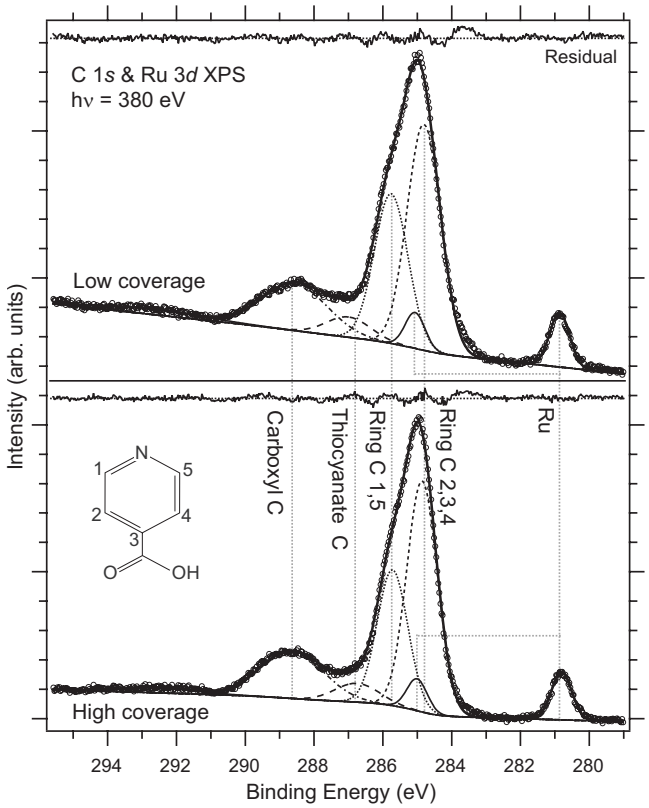

FIG. 7. C 1*s* core-level photoemission spectra measured using $h\nu$ =380 eV. Total instrument resolution was <110 meV.

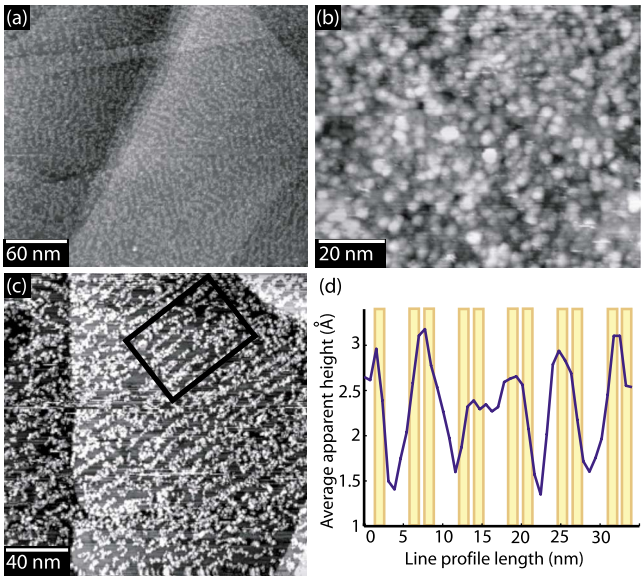

FIG. 8. (Color online) STM images of N3 deposited onto the mica-supported Au(111) reconstruction. (a) Submonolayer N3 coverage (V_{sample} = +2.50 V, I_{tunnel}=0.03 nA, 300×258 nm^2). (b) Monolayer N3 coverage (V_{sample} = +2.50 V, I_{tunnel}=0.03 nA, 100×79 nm^2). (c) Submonolayer N3 coverage (V_{sample} = +2.50 V, I_{tunnel}=0.03 nA, 200×200 nm^2) indicating an area for which the average height profile is shown in (d). The maxima of the Au(111) herringbone reconstruction undulations are also shown superimposed in (d).

The most intense peak in the spectrum at ~285 eV is mainly due to C atoms in the pyridine ring. Here we can resolve those ring C atoms that neighbor a N atom (atoms 1 and 5 in Fig. 7) and those that do not (atoms 2, 3, and 4). These components were additionally constrained to have the same FWHM, placing them at BEs of ~285.8 and ~284.8 eV, respectively. This resolution of two peak components for the ring C was found previously using angle-resolved XPS of isonicotinic acid on TiO_2,[25] which allowed identification of each peak.

The peak at 288.6 eV is due to carboxyl C atoms and the remaining peak at ~286.9 eV is due to thiocyanate C atoms. Based on the stoichiometry of the N3 molecule, the ratio of (2,3,4)pyridine:(1,5)pyridine:carboxyl:thiocyanate C atoms for N3 is 6:4:2:1. Here the ratios found were 6.0:4.0:2.4:0.7 and 6.0:4.0:2.5:0.7 for the low and high coverages, respectively. The feature at ~292 eV is a shake-up.

Figure 8 shows the STM images of N3 deposited onto the mica-supported Au(111) surface. Large area scans of the surface with low molecular coverage, such as the example shown in Fig. 8(a), reveal that N3 adsorbs preferentially to produce a herringbone pattern mimicking that of the underlying substrate reconstruction. The characteristic Au(111) herringbone reconstruction[22] is easily identifiable in STM and consists of pairs of bright lines which bend through 120° and follow the $[11\bar{2}]$ crystallographic axis of the surface. The adsorbed molecules reproduce the morphological features of the herringbone reconstruction with a broad row of molecules being imaged in place of the two bright lines normally observed. As the coverage is increased up to a full monolayer the bare Au regions between the lines are filled in to produce a molecular overlayer with no discernable long range order [shown in Fig. 8(b)]. The lack of three-dimensional island growth during the submonolayer to monolayer growth regime indicates that the molecule-substrate interaction (mediated by the S–Au interaction) dominates over the molecule-molecule interaction, and that molecules impinging upon the surface are free to diffuse. Figure 8(c) shows a region of low coverage, where the section enclosed by the marked rectangle has been analyzed in Fig. 8(d), showing the mean of the line profiles taken widthwise across the rectangle. The expected periodicity of the herringbone reconstruction has been superimposed upon the averaged line profile demonstrating a good agreement with the observed position of the molecular rows and confirming their similar periodicity. Measurement of the apparent height of the periodic features facilitates the discrimination between clean Au(111) and low coverage regions of the surface. The undulation of the herringbone is 0.2 A, an order of magnitude smaller than that of the adsorbed molecules, making it possible to determine that the region shown in image 8(a) contains adsorbed molecules ordered by the Au(111) reconstruction.

The XPS and STM data together describe how N3 adsorbs to the Au(111) surface. The XPS spectra show that N3 bonds to Au via the S atoms of the thiocyanate ligands, most likely accompanied by a physisorption interaction from the bi-isonicotinic acid ligands. The different components in the S 2*p* spectra imply that S atoms bond to at least two types of Au(111) adsorption site, and that they may also bond to S atoms of neighboring N3 molecules at the Au surface. STM images indicate that the N3 molecules adsorb preferentially to the faulted regions of the Au(111) herringbone reconstruction. These are areas of high electron density, so it is perhaps unsurprising that S atoms interact most strongly here.

Previous experiments have shown that the HOMO of N3 is located on the thiocyanate ligands.[1,5,6] For N3 adsorbed on Au then, this places the HOMO of N3 on the part of the molecule chemically bound to the Au surface. Thus, in a solid state DSC the HOMO would be ideally located to receive electrons from the Au, replacing those electrons lost through the HOMO-LUMO photoexcitation and subsequent charge injection into the TiO_2. Additionally, in a DSC where the Au atoms form islands/networks on the TiO_2 surface, N3 molecules could also bond to the TiO_2 via at least one bi-isonicotinic acid ligand,[6,26] ideally placing the LUMO for electron injection.

IV. CONCLUSIONS

The adsorption of the dye molecule N3 on the Au(111) surface using UHV electrospray deposition has been studied using XPS and STM. The XPS data, in particular the S 2*p* spectra, have been interpreted to conclude that N3 bonds to Au(111) via S atoms and adsorbs preferentially at the faulted regions of the Au(111) herringbone reconstruction. This is fundamental to understanding the use of N3 in a solid state DSC that uses a metallic electrode such as Au to replenish electrons lost by the dye. Further studies are currently underway to probe the charge transfer interaction between N3 and the Au surface.

ACKNOWLEDGMENTS

We are grateful for financial support by the European Community-Research Infrastructure Action under the FP6 "Structuring the European Research Area" Programme (through the Integrated Infrastructure Initiative "Integrating Activity on Synchrotron and Free Electron Laser Science"), the UK Engineering and Physical Sciences Research Council (EPSRC) through Grant Nos. GR/R91953/01 and EP/D048761/01, Vetenskapsrådet, and the European Commission through the Early Stage Researcher Training Network MONET (Grant No. MEST-CT-2005-020908). We express our thanks to the staff of MAX-lab for their technical assistance. We would also like to acknowledge Dr. J. B. Taylor and Dr. J. C. Swarbrick for their developmental work on previous electrospray apparatus and Professor P. H. Beton for access to the UHV STM.

[1] A. Hagfeldt and M. Grätzel, Acc. Chem. Res. **33**, 269 (2000).
[2] M. Grätzel, Nature (London) **414**, 338 (2001).
[3] M. Grätzel, J. Photochem. Photobiol. C **4**, 145 (2003).
[4] M. Grätzel, J. Photochem. Photobiol., A **164**, 3 (2004).
[5] H. Rensmo, S. Lunell, and H. Siegbahn, J. Photochem. Photobiol., A **114**, 117 (1998).
[6] L. C. Mayor, J. B. Taylor, G. Magnano, A. Rienzo, C. J. Satterley, J. N. O'Shea, and J. Schnadt, J. Chem. Phys. **129**, 114701 (2008).
[7] E. W. McFarland and J. Tang, Nature (London) **421**, 616 (2003).
[8] M. Grätzel, Nature (London) **421**, 586 (2003).
[9] L. Patthey, H. Rensmo, P. Persson, K. Westermark, L. Vayssieres, A. Stashans, Å. Petersson, P. A. Brühwiler, H. Siegbahn, S. Lunell, and N. Mårtensson, J. Chem. Phys. **110**, 5913 (1999).
[10] P. Persson, S. Lunell, P. A. Brühwiler, J. Schnadt, S. Södergren, J. N. O'Shea, O. Karis, H. Siegbahn, N. Mårtensson, M. Bässler, and L. Patthey, J. Chem. Phys. **112**, 3945 (2000).
[11] J. N. O'Shea, Y. Luo, J. Schnadt, L. Patthey, H. Hillesheimer, J. Krempaský, D. Nordlund, M. Nagasono, and N. Mårtensson, Surf. Sci. **486**, 157 (2001).
[12] J. N. O'Shea, J. Schnadt, P. A. Brühwiler, and H. H. N. Mårtensson, J. Phys. Chem. B **105**, 1917 (2001).
[13] J. N. O'Shea, J. C. Swarbrick, K. Nilson, C. Puglia, B. Brena, Y. Luo, and V. Dhanak, J. Chem. Phys. **121**, 10203 (2004).
[14] J. B. Taylor, L. C. Mayor, J. C. Swarbrick, J. N. O'Shea, C. Isvoranu, and J. Schnadt, J. Chem. Phys. **127**, 134707 (2007).
[15] J. B. Taylor, L. C. Mayor, J. C. Swarbrick, J. N. O'Shea, and J. Schnadt, J. Phys. Chem. C **111**, 16646 (2007).
[16] G. J. Kluth, C. Carraro, and R. Maboudian, Phys. Rev. B **59**, R10449 (1999).
[17] P. Fenter, A. Eberhardt, and P. Eisenberger, Science **266**, 1216 (1994).
[18] C. J. Satterley, L. M. A. Perdigao, A. Saywell, G. Magnano, A. Rienzo, L. C. Mayor, V. R. Dhanak, P. H. Beton, and J. N. O'Shea, Nanotechnology **18**, 455304 (2007).
[19] A. Saywell, G. Magnano, C. J. Satterley, L. M. A. Perdigão, N. R. Champness, P. H. Beton, and J. N. O'Shea, J. Phys. Chem. C **112**, 7706 (2008).
[20] R. Denecke, P. Vaterlein, M. Bassler, N. Wassdahl, S. Butorin, A. Nilsson, J. E. Rubensson, J. Nordgren, N. Mårtensson, and R. Nyholm, J. Electron Spectrosc. Relat. Phenom. **101–103**, 971 (1999).
[21] I. Horcas, R. Fernandez, J. Gomez-Rodriguez, J. Colchero, J. Gomez-Herrero, and A. Baro, Rev. Sci. Instrum. **78**, 013705 (2007).
[22] J. V. Barth, H. Brune, G. Ertl, and R. J. Behm, Phys. Rev. B **42**, 9307 (1990).
[23] J. A. Rodriguez, J. Dvorak, T. Jirsak, G. Liu, J. Hrbek, Y. Aray, and C. González, J. Am. Chem. Soc. **125**, 276 (2003).
[24] J. C. Fuggle and N. Mårtensson, J. Electron Spectrosc. Relat. Phenom. **21**, 275 (1980).
[25] J. Schnadt, J. N. O'Shea, L. Patthey, J. Schiessling, J. Krempaský, M. Shi, N. Mårtensson, and P. A. Brühwiler, Surf. Sci. **544**, 74 (2003).
[26] E. M. J. Johansson, M. Hedlund, H. Siegbahn, and H. Rensmo, J. Phys. Chem. B **109**, 22256 (2005).